

Quantum kinetic theory VII: The influence of vapor dynamics on condensate growth

M. J. Davis¹, C. W. Gardiner², and R. J. Ballagh³

¹Clarendon Laboratory, Department of Physics, University of Oxford, United Kingdom.

²School of Chemical and Physical Sciences, Victoria University of Wellington, New Zealand

³Physics Department, University of Otago, Dunedin, New Zealand

October 16, 2019

We extend earlier models of the growth of a Bose-Einstein condensate [1–3] to include the full dynamical effects of the thermal cloud by numerically solving a modified quantum Boltzmann equation. We determine the regime in which the assumptions of the simple model are a reasonable approximation, and compare our new results with those that were earlier compared with experimental data. We find good agreement with our earlier modelling, except at higher condensate fractions, for which a significant speedup is found. We also investigate the effect of temperature on condensate growth, and find that this has a surprisingly small effect.

The discrepancy between theory and experiment remains, since the speedup found in these computations does not occur in the parameter regime specified in the the experiment.

I. INTRODUCTION

The fundamental process in the growth of a Bose-Einstein condensate is that of *bosonic stimulation*, by which atoms are scattered into and out of the condensate at rates enhanced by a factor proportional to the number of atoms in the condensate. This was first quantitatively considered by Gardiner *et al.* [1], in a paper which treated the idealized case of the growth of a condensate from an nondepletable “bath” of atoms at a fixed positive chemical potential and temperature T . This gave rise to a simple and elegant formula known as the *simple growth equation*

$$n_0 = 2W^+(n_0) \frac{n}{1 - e^{[c(n_0)]/kT}} \stackrel{\circ}{n_0 + 1} ; \quad (1)$$

in which n_0 is the population of the condensate, c is the chemical potential of the thermal cloud, and $c(n_0)$ is the condensate eigenvalue. The prefactor $W^+(n_0)$ is a rate with an expression derived from quantum kinetic theory [4], which was estimated approximately in [1] by using a classical Boltzmann distribution. To go beyond the Boltzmann approximation for W^+ involves a very much more detailed treatment of the populations of the trap levels with energy less than c , since the equilibrium Bose-Einstein distribution for $E > 0$ is not consistent with energies less than c . In other words, the populations of the lower trap levels *cannot* be treated as time-independent, and thus the dynamics of growth must include at least this range of trap levels as well as the condensate level. Therefore in [2,3] we considered a less simplified model, covering a range of energies up to a cut-off, E_R , above which the system was assumed to be a thermal cloud with a fixed temperature and chemical potential. Equations were derived for the rate of growth of these levels along with the condensate, and the rates at which particles from the thermal bath scattered these quasi-particles between levels within the condensate band. The results of calculations showed that a speedup

of the growth rate by a factor of the order of 3–4 compared to the simple growth equation could be expected, and that the initial part of the growth curve would be modified, leading to a much sharper onset of the initiation of the condensate growth.

The only experiment that has been done on condensate growth [11] was then under way. In these experiments clouds of sodium atoms were cooled to just above the transition temperature, at which point the high energy tail of the distribution was rapidly removed by a very severe RF “cut”, where the frequency of the RF field was quickly ramped down. After a short period of equilibration, the resulting vapor distribution was found to be similar to the assumptions of our theoretical treatments, and condensate growth followed promptly. The results obtained were fitted to solutions of the simple growth equation (1). When experimental results became available a speedup of about the predicted factor was found, and indeed the higher temperature results agreed very well with the theoretical predictions. At lower temperatures there was still some disparity; the theory predicted a slower rate of growth with decreasing temperature, but experimentally the opposite was observed.

The situation in which we now find ourselves leaves no alternative other than to address the remaining approximations. In our previous work we have made four major approximations:

- i) The part of the vapor with energies higher than E_R has been treated as being time independent.
- ii) The energy levels above the condensate level were modified phenomenologically to account for the fact that they must always be greater than the condensate chemical potential, which rises as the condensate grows.
- iii) We treated all levels as being particle-like, on the grounds that detailed calculations [12] have shown that only a very small proportion of excitations of a trapped Bose gas are not of this kind.

iv) We have used the quantum Boltzmann equation in a ergodic form, in which all levels of a similar energy are assumed to be equally occupied.

In this paper we will no longer require the first two of these approximations. Abandoning the first means that we are required to take care of all kinds of collisions which can occur, and thus treat the time-dependence of all levels. This comes at a dramatic increase in both the computation time required (hours rather than seconds) and the precision of algorithms required. We also use a density of states which should be close to the actual density of states as the condensate grows, thereby avoiding the phenomenological modification of energy levels. However, we still treat all of the levels as being particle-like, since it seems unlikely that the few non-particle-like excitations will have very little effect on the growth as a whole. The ergodic form of the quantum Boltzmann is needed to make the computations tractable, and is of necessity retained.

II. FORMALISM

The basis of our method is Quantum Kinetic theory, a full exposition of which is given in Ref. [4]. These develop a complete framework for the study of a trapped Bose gas in a set of master equations. The full solution of these equations is not

$$g'' \frac{\partial f''}{\partial t} = \frac{8m a^2}{h^3} \sum_{n_1, n_2, n_3} X () g'' f f_1 f_2 (1 + f_3) [1 + f''] (1 + f_1) (1 + f_2) f_3 f'' g : \quad (2)$$

Here f'' is the distribution function of the gas, and g'' is the density of states, given by $g'' = n^2 = (2h^3)^3 x^3 y^3 z^3$ for the ideal gas in a harmonic trap. We also define $= n_1 + n_2 + n_3$, and $n_{\text{min}} = \min(n_1, n_2, n_3)$, and use the shorthand notation $f_1 = f(n_1)$ etc. The MQBE is the basis of our computer simulations.

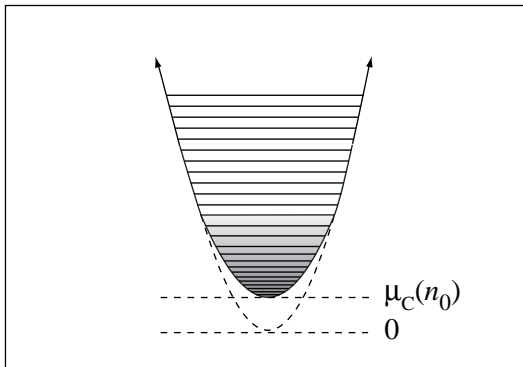


FIG. 1. Qualitative picture of the compression of the quantum levels above the condensate mode as the condensate eigenvalue increases.

feasible, however, and therefore some type of approximation must be made. The basic structure of the method used here is essentially the same as that of QKVI, the major difference being that all time-dependence of the distribution function is retained. As explained in [3,10], quantum kinetic theory leads to a model which can be viewed as a modification of the quantum Boltzmann equation in which

- i) The condensate wavefunction and energy eigenvalue—the condensate chemical potential $\mu_c(n_0)$ —are given by the solution of the time-independent Gross-Pitaevskii equation with n_0 atoms.
- ii) The trap levels above the condensate level are the quasi-particle levels appropriate to the condensate wavefunction. This leads to a density of states for the trap levels which is substantially modified, as discussed below in Sect.III B
- iii) The transfer of atoms between levels is given by a modified quantum Boltzmann equation (MQBE) in the energy representation. This makes the ergodic assumption; that the distribution function depends only on energy.

In this approximation, the MQBE takes the form [14]

III. DETAILS OF MODEL

The most important aspect of our model is the inclusion of the mean field effects of the condensate. As the population of the condensate increases, the absolute energy of the condensate level also rises due to the atomic interactions. This results in a compression in energy space of the quantum levels immediately above the condensate, (see Fig. 1) and has an important effect on the evolution of the cloud.

The correct description of the quantum levels immediately above the ground state when there is a significant condensate population requires a quasiparticle transformation. This is computationally difficult, however, so we make use of a single-particle approximation for these states. This should be reasonable, as most of the growth dynamics will involve higher lying states that will be almost unaffected by the presence of the condensate. In [3] we did this using a linear interpolation of the density of states; here we use an approximate treatment based on the Thomas-Fermi approximation.

A. Condensate chemical potential $\mu_c(n_0)$

We consider a harmonic trap with a geometric mean frequency of

$$! = (\mathbf{!}_x \mathbf{!}_y \mathbf{!}_z)^{1=3}; \quad (3)$$

We include the mean field effects via a Thomas-Fermi approximation for the condensate eigenvalue, which is directly related to the number of atoms in the condensate mode. As in [3,10], we use a modified form of this relation in order to give a smooth transition to the correct harmonic oscillator value when the condensate number is small:

$$c(n_0) = \frac{h}{n_0 + (3h! = 2)^{5=2}}; \quad (4)$$

where $= (15a! m^{1=2} n^2 = 4 \frac{p}{2})^{2=5}$. Thus, for $n_0 = 0$ we have $c(0) = "0 = 3 = 2h!$.

B. Density of states $g(")$

We assume a single particle energy spectrum with a Bogoliubov-like dispersion relation, as in Timmermans *et al.* [13], which leads to a density of states of the form

$$g(") = \frac{4}{(h!)^3} \frac{c(n_0)^2}{6} \frac{h}{c(n_0)} \int_0^{\infty} dx \frac{p}{1-x} \frac{h_p}{p} \frac{\frac{h_p}{(" = c(n_0))^{1/2} + x^2}}{\frac{h_p}{(" = c(n_0))^{1/2} + x^2}} + \frac{h_p}{x} \frac{\frac{h_p}{(" = c(n_0))^{1/2} + x^2}}{\frac{h_p}{(" = c(n_0))^{1/2} + x^2}} + \frac{h_p}{x} \frac{r}{p} \frac{r}{x} \frac{h}{c(n_0)} \frac{3}{x^5}; \quad (5)$$

This integral can be carried out analytically; the result is

$$g(") = \frac{h^2}{2(h!)^3} \left(1 + q_1(c(n_0) = ") + \frac{1}{"} \frac{c(n_0)}{"}^2 q_2 \frac{1}{(" = c(n_0))^{1/2}} \right); \quad (6)$$

where

$$q_1(x) = \frac{2}{p} \frac{p}{x} \frac{p}{1-x} (1-2x) \sin^{-1} \left(\frac{p}{x} \right); \quad (7)$$

$$q_2(x) = \frac{4}{p} \frac{p}{2} \frac{p}{2x+x \log \frac{1+x}{p} \frac{p}{1+x^2}} \frac{1+x}{2} + \sin^{-1} \frac{x}{p} \frac{1}{1+x^2}; \quad (8)$$

This is plotted in Fig. 2, along with that for the ideal gas. Thus the density of states of the trap varies smoothly as the condensate grows.

IV. NUMERICAL METHODS

A. Representation

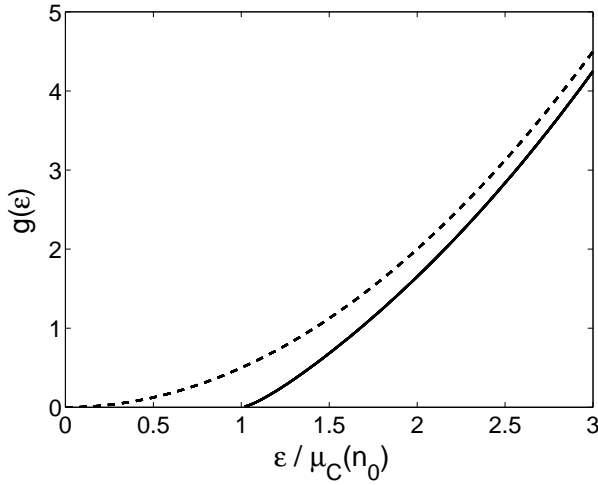


FIG. 2. The modified density of states (solid curve) compared with non-interacting function (dashed curve) for the harmonic trap.

We represent the distribution function $f(")$ by a series of energy bins, divided into two distinct regions, as shown diagrammatically in Fig. 3. The lowest energy region corresponds essentially to the *condensate band* R_C of [1,3,7,10]. This is the region in which $f(")$ is rapidly varying in the regime of quantum degeneracy, and is described by a series of fine-grained energy bins up to an energy $E_R = 3 c(n_{0, \text{max}})$. The condensate is a *single* quantum state represented by the lowest energy bin. The n th bin above the condensate level within R_C represents several quantum levels about an energy of $"_n$. The range of each bin is typically $"_n = 5h!$, and contains $g("n)$ $"_n$ levels. As the condensate grows, these energy bins are compressed, and their widths decrease to take account of the fact of the increasing condensate eigenvalue.

This compression occurs very slowly on the time scale of the simulations, and we keep the number of particles in each bin $g("n) f("n) = "n$ constant for the adjustment. The change in the value of $f("n)$ due to this compression is very much smaller than any change due to the growth dynamics during the time step, so this seems a reasonable approach.

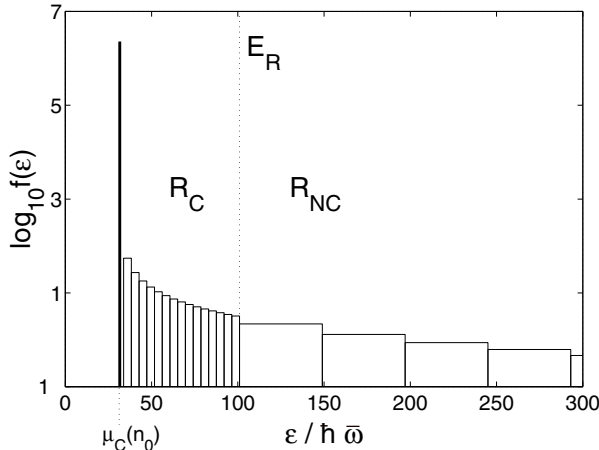


FIG. 3. The numerical representation of the system with a condensate of 2.3×10^6 atoms at a temperature of 530nK. R_C is the condensate band, which is fine-grained, whereas R_{NC} is the non-condensate band, which is coarse-grained. The division between the two bands is fixed at E_R . The condensate energy is derived from the Thomas-Fermi approximation.

The high energy region corresponds to the *thermal bath* of our previous papers. This is the region in which $f(\epsilon)$ is slowly varying in ϵ , and therefore the energy bins are considerably broader (up to $64\hbar\omega$ in the results presented in this paper). The evaporative cooling is numerically carried out by the sudden removal of population of the bins in this region with $n > n_{cut}$.

B. Solution

There are four different types of collision that can occur given our numerical description of the system. These are depicted in Fig. 4.

- (a) *Growth*: This involves two particles in R_{NC} colliding, resulting in the transfer of one of the particles to the condensate band (along with the reverse process).
- (b) *Scattering*: A particle in R_{NC} collides with a particle in the condensate band, with one particle remaining in R_C .
- (c) *Internal*: Two particles within the condensate band collide with at least one of these particles remaining in R_{NC} after the collision.
- (d) *Thermal*: This involves all particles involved in the collision coming from the non-condensate band and remaining there.

Our first description of condensate growth [1] considered only process (a). The next calculation [2,3] involved both process (a) and (b). The calculations presented below include all four processes, allowing us to determine whether the earlier approximations were justified.

The computation of the rates of processes (a) and (b) is made difficult because of the different energy scales of the two regions of the distribution function. Our solution to this is to *interpolate* the distribution function $f(\epsilon)$ in R_{NC} (non-condensate band) such that the bin sizes are reduced to be the same as for R_C (the condensate band). The rates are then calculated using this interpolated distribution function, now consisting of more than one thousand bins, and the rates for the large bins of the non-condensate band are found by summing the rates of the appropriate interpolated bins.

We have found that these rates are *extremely* sensitive to the accuracy of the numerical interpolation — small errors lead to inconsistencies in the solutions of the MQBE. This procedure is more efficient than simply using the same bin size for the whole distribution, as there are only a small number of bins for the condensate band.

The method has been tested by altering the position of E_R and width of the energy bins of R_{NC} . We have found that the solution is independent over a large range of values of these parameters.

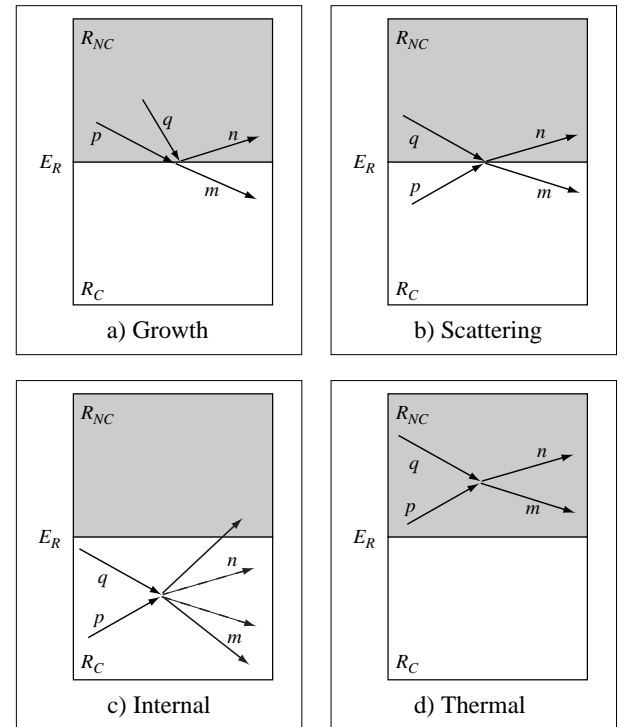


FIG. 4. The four different collision types that can occur in our numerical description.

V. RESULTS

In this paper we present the results of simulations modelling the experiments described in [11]. In these experiments a cloud of sodium atoms confined in a ‘cigar’ shaped magnetic trap was evaporatively cooled to just above the Bose-Einstein transition temperature. Then, in a period of 10ms the high energy tail of the distribution was removed with a very rapid and

rather severe RF cut. The condensate was then manifested by the formation of a sharp peak in the density distribution.

We have carried out a full investigation of the effect of varying the initial cloud parameters has on the growth of the condensate for the trap configuration described in [11]. In this paper we concentrate on a comparison of these results with our earlier theoretical model. To model these experiments, we begin our simulations with an equilibrium Bose-Einstein distribution, with temperature T_i and chemical potential μ_{init} and truncate it at an energy $\epsilon_{\text{cut}} = kT_i$, which represents the system at the end of the RF sweep. This is then allowed to evolve in time, until the gas once again approaches an equilibrium the appropriate equilibrium Bose-Einstein in the presence of a condensate. This is pictured schematically in Fig. 5

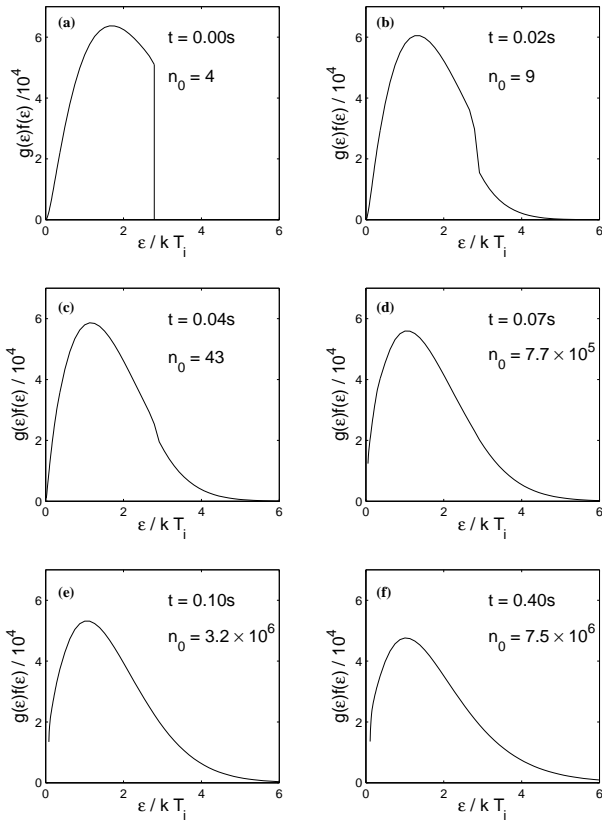


FIG. 5. Snapshots of the distribution function for a simulation with initial conditions $\mu_{\text{init}} = 100\hbar\omega$, $T_i = 1119nK$, and $\omega = 2.83$. This results in a condensate with $n_0 = 7.5 \times 10^6$ atoms at a temperature of $T_f = 830nK$. For clarity, the condensate itself is not depicted, but the presence of a significant amount of condensate has the effect of displacing the left hand ends of the curves (d)–(f) an amount $\mu_{\text{init}} = kT_i$ from the axis. The growth curve for this simulation is shown in Fig. 6.

Because of the ergodic assumption, the MQBE that we simulate depends only on the geometric average of the trapping frequencies $\omega = (\omega_x \omega_y \omega_z)^{1/3}$. There is likely to be some type of experimental dependence on the actual trap geometry which is not included in our simulation; however in the regime $kT \ll \hbar\omega$ this should be small. The trap parameters

of [11] were $(\omega_x, \omega_y, \omega_z) = (82.3, 82.3, 18)Hz$, giving $\mu_{\text{init}} = 2.496Hz$.

A. Matching the experimental data

The main source of quantitative experimental data of condensate growth generally available is Fig. 5 of [11]. This gives growth rates as a function of final condensate number and temperature rather than the initial conditions. Whereas the growth curves calculated in [1,3] required these parameters as inputs, the calculations presented here require three input parameters; the initial number of atoms in the system N_i (and hence the initial chemical potential μ_{init}), the initial temperature T_i , and the position of the cut energy $\epsilon_{\text{cut}} = kT_i$.

Given the final parameters supplied in [11], it is possible to calculate a set of initial conditions that we require. As we know the final condensate number, we can calculate the value of the chemical potential of the gas using the Thomas-Fermi approximation for the condensate eigenvalue. This gives a density of states according to Eq. 6, and along with the measured final temperature T_f , we can calculate the total energy E_{tot} and number of atoms N_{tot} in the system at the end of the experiment, completely characterizing the final state of the gas.

$$N_{\text{tot}} = n_0 + \sum_{n > \mu_{\text{init}}(n_0)} \frac{g(n)}{\exp[(\epsilon_n - \mu_{\text{init}}(n_0))/kT_f]} \quad (9)$$

$$E_{\text{tot}} = E_0(n_0) + \sum_{n > \mu_{\text{init}}(n_0)} \frac{n g(n)}{\exp[(\epsilon_n - \mu_{\text{init}}(n_0))/kT_f]} \quad (10)$$

We now want to find an initial distribution that would have the same total energy and number of atoms if truncated at $\epsilon_{\text{cut}} = kT_i$. If we specify an initial chemical potential for the distribution μ_{init} , we can self-consistently solve for the parameters T_i and μ_{init} from the following non-linear set of equations

$$N_{\text{tot}} = \sum_{n=3-2h}^{\mu_{\text{init}}(n_0)} \frac{g(n)}{\exp[(\epsilon_n - \mu_{\text{init}})/kT_i]} \quad (11)$$

$$E_{\text{tot}} = \sum_{n=3-2h}^{\mu_{\text{init}}(n_0)} \frac{n g(n)}{\exp[(\epsilon_n - \mu_{\text{init}})/kT_i]} \quad (12)$$

This gives the input parameters for our simulation, and we can now calculate growth curves starting with initially different clouds, but resulting in the same final condensate number and temperature.

B. Typical results

A sample set of growth curves is presented in Fig. 6a, for a condensate with 7.5×10^6 atoms at a temperature of $830nK$

and a condensate fraction of 10.4%. The initial value parameters for the curves are given in Table I. We find that for $\text{init} > 100\text{h!}$, the growth curves are identical to the naked eye.

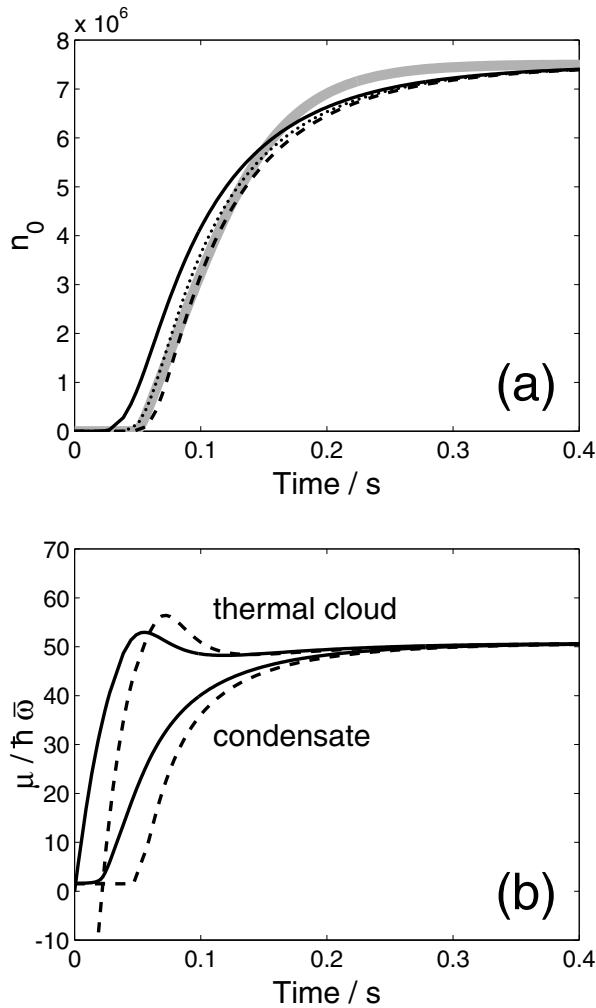


FIG. 6. Growth of a condensate with $n_0 = 7.5 \times 10^6$, $T_f = 830\text{nK}$. Solid lines $\text{init} = 0$, dotted lines $\text{init} = 40\text{h!}$, dashed lines $\text{init} = 100\text{h!}$: (a) Population of condensate versus time. Grey curve is the solution for model of [3]. (b) Chemical potential $\mu_c(n_0)$ of condensate (lower curves) and effective chemical potential μ_e of thermal cloud (upper curves).

$\text{init} = \text{h!}$	$T_i (\text{nK})$	$N_i = 10^6$	$\mu_{\text{cut}} = \text{h!}$
0	1000	89.1	3.82
-40	1080	100.1	3.31
-100	1119	117.6	2.83

TABLE I. Parameters for the formation of a condensate with $n_0 = 7.5 \times 10^6$ atoms at a temperature of $T_f = 830\text{nK}$ from an uncondensed thermal cloud. The growth curves are plotted in Fig. 6

As can be seen the curves are very similar, and arguably would be difficult to distinguish in experiment. The main

difference is the further the system starts from the transition point (i.e. the more negative the initial chemical potential), the longer the initiation time but the steeper the growth curve.

1. Effective chemical potential

To facilitate understanding of these results, we introduce the concept of an effective chemical potential μ_e for the non-condensate band. We do this by fitting a Bose-Einstein distribution to the lowest energy bins of R_{NC} as a function of time. Obviously, there is no defined chemical potential when the system is not in equilibrium, but as has been noted for the classical Boltzmann equation [15], the distribution function tends to resemble an equilibrium distribution as evaporative cooling proceeds. The effective chemical potential is not unique—it is dependent on the particular choice of the energy cutoff E_R , but it gives a good indication of the “state” of the non-condensate, since the majority of the growth comes from the lower bins during the initiation of the condensate. In this paper μ_e was computed by fitting a straight line to $\log[1 + 1 = f(\mu)]$ in the first 10 bins of the noncondensate band distribution, with the intercept giving μ_e and the gradient the temperature.

2. Interpretation

We find that all the results presented in this paper can be qualitatively understood in terms of the simple growth equation Eq. (1), with the vapour chemical potential μ_c replaced by the effective chemical potential μ_e of the thermal cloud.

The simple growth equation requires $\mu_e > \mu_c(n_0)$ for condensate growth to occur. In Fig. 6b we plot the effective chemical potential μ_e of the thermal cloud and the chemical potential of condensate $\mu_c(n_0)$, and these explain the two effects noted above—longer initiation time and steeper growth. Firstly, the inversion of the chemical potentials for the simulation with $\text{init} = 100\text{h!}$ occurs at a later time than for $\text{init} = 0$, causing the growth curve to begin later. This is because the initial cloud for the $\text{init} = 100\text{h!}$ case is further from the transition point at $t = 0$. Secondly, the effective chemical potential of the thermal cloud rises more steeply, meaning that $\mu_e - \mu_c(n_0)$ is larger, and therefore the rate of condensate growth is increased.

C. Comparison with earlier model

In Fig. 6a we have also plotted the growth curve that is predicted by the model of [3]. For this earlier model this model the initial condensate number is indeterminate, whereas for the detailed calculation presented here the distribution is initially a Bose-Einstein distribution, and the zero of the time axis is determined by the removal of the high energy tail.

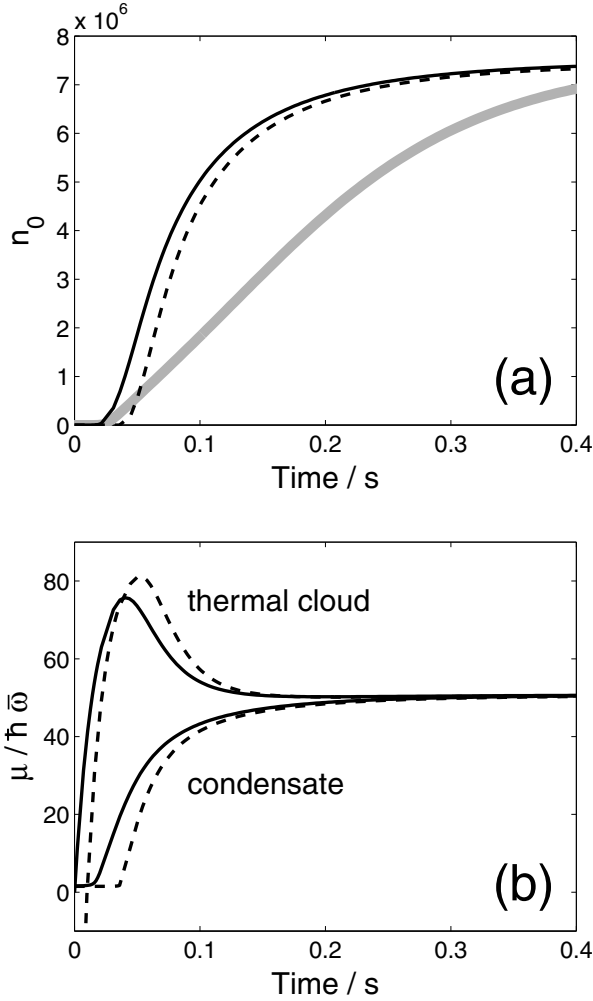


FIG. 7. Comparison of condensate growth models for a condensate fraction of 24.1%, $n_0 = 7.5 \times 10^6$, $T_f = 590\text{nK}$. Solid lines $\text{in} \ddot{\text{u}} \text{t} = 0\text{h}!$, dashed lines $\text{in} \ddot{\text{u}} \text{t} = 100\text{h}!$: (a) Population of condensate versus time. Grey line is the solution for model of [3]. (b) Chemical potential of condensate (lower curves) and effective chemical potential of thermal cloud (upper curves).

For these particular parameters, it turns out that the results of the full calculation of the growth curve give very similar results to the previous model, with the initial condensate number adjusted appropriately. This is not surprising; indeed, from Fig. 6b we can see that the approximation of the thermal cloud by a constant chemical potential (ie the cloud is not depleted) is good for the region where the condensate becomes macroscopic.

For larger condensate fractions, however, the principal condition assumed in the model of [3], that the chemical potential of the vapor can be treated as approximately constant, is no longer satisfied. In Fig 7a we plot the growth of the same size condensate as in Fig 6, (that is, 7.5×10^6 atoms) but at a lower final temperature of 590nK. In this situation the condensate fraction increases to 24.1%, and so there is considerable depletion of the thermal cloud. The effect of this can be seen in Fig. 7b. The difference between the vapor and condensate chemical potentials $\mu_e - \mu_c(n_0)$ increases to very large val-

ues before any appreciable condensate fraction appears. The onset of significant condensate growth then begins to deplete the thermal cloud, so that μ_e then begins to decrease. Because the condensate fraction is large, μ_e must decrease significantly from its maximum value in order to accommodate the loss of atoms from the vapor. This means that the growth rate is significantly enhanced, because the typical value of difference $\mu_e - \mu_c(n_0)$ during the growth stage is very large.

This results in an increased growth rate compared to the model of [3], which fixes the chemical potential of the thermal cloud at a constant value, and cannot take into account this ‘overshoot’ of the chemical potential arising from thermal cloud dynamics.

D. Effect of the final temperature on condensate growth

We have investigated the effect that final temperature has on the growth of a condensate of a fixed number. All simulations were chosen with $\text{in} \ddot{\text{u}} \text{t} = 0$, since the initial chemical potential has little effect on the overall shape of the growth curves, with varying initial temperatures and cut parameters. The initial conditions are shown in Table II, while the results are presented in Fig. 8.

We see the somewhat surprising result that the growth curves do not change significantly over a very large temperature range for the same size condensate. In fact, a condensate formed at 400nK grows more quickly than at 600nK for these parameters. As the temperature is increased further, however, the growth rate increases again, and at a final temperature of 1 K the growth rate is faster than at 400nK. This effect has also been observed for both larger (7.5×10^6) and smaller (1×10^6) condensates.

This observation can once again be interpreted using the simple growth equation Eq. 1. Although $W^+(n_0)$ increases with temperature (approximately as T^2 as shown in [1]), the difference in the chemical potentials of the condensate and the thermal cloud decreases, as the evaporative cooling cut required is less severe and the final condensate fraction is lower. Also, the term in the curly brackets of Eq. 1 is also approximately proportional to T^{-1} for most regimes. The end result is that the decrease in this term compensates for the increase in $W^+(n_0)$, giving growth curves that are very similar. Once the ‘overshoot’ of the thermal cloud chemical potential ceases to occur (when the evaporative cooling cut is not as severe), the growth rate begins to increase with temperature as predicted by the model of [3].

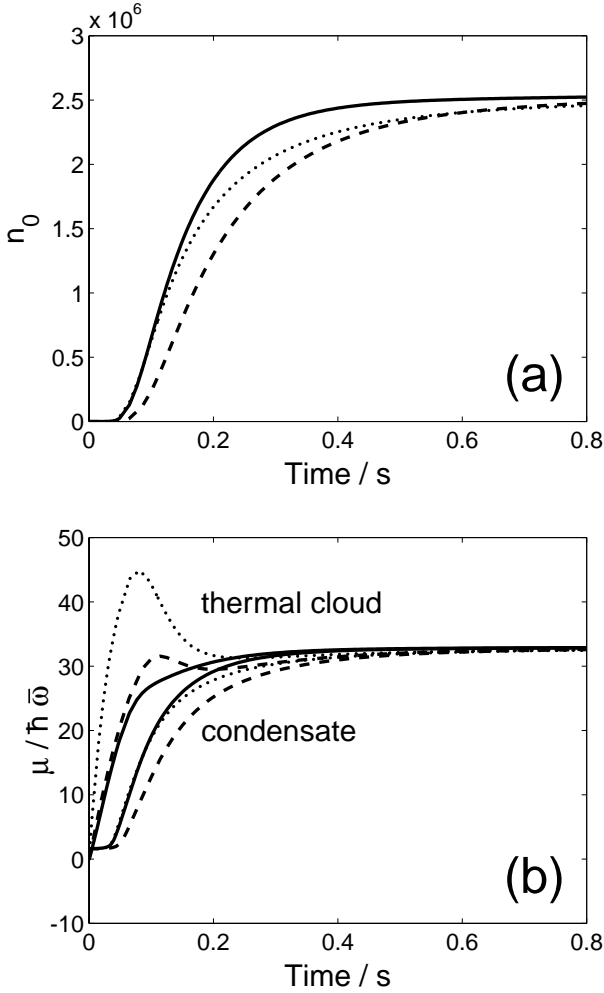


FIG. 8. Growth of a condensate with a final condensate size of 2.5×10^6 atoms. The dotted line is for a final temperature of 400nK, dashed 600nK, and solid 1 K.

T_f (nK)	T_i (nK)	$N_i = 10^6$	$"_{cut}=h!$	Condensate fraction
400	622.0	21.5	2.19	0.253
600	707.3	31.6	4.03	0.099
1000	1064.8	107.7	5.87	0.025

TABLE II. Parameters for the formation of condensate with $n_0 = 2.5 \times 10^6$ atoms from an uncondensed thermal cloud with $_{init} = 0$. The growth curves are presented in Fig. 8

E. Effect of size on condensate growth

Finally we have performed some simulations of the formation of a condensate at a fixed final temperature, but of a varying size. The parameters for these simulations are given in Table III, and the growth curves are plotted in Fig. 9a. We find that the larger the condensate, the more rapidly it grows. The initial clouds required to form the larger condensates not only start at a higher temperature (and thus have

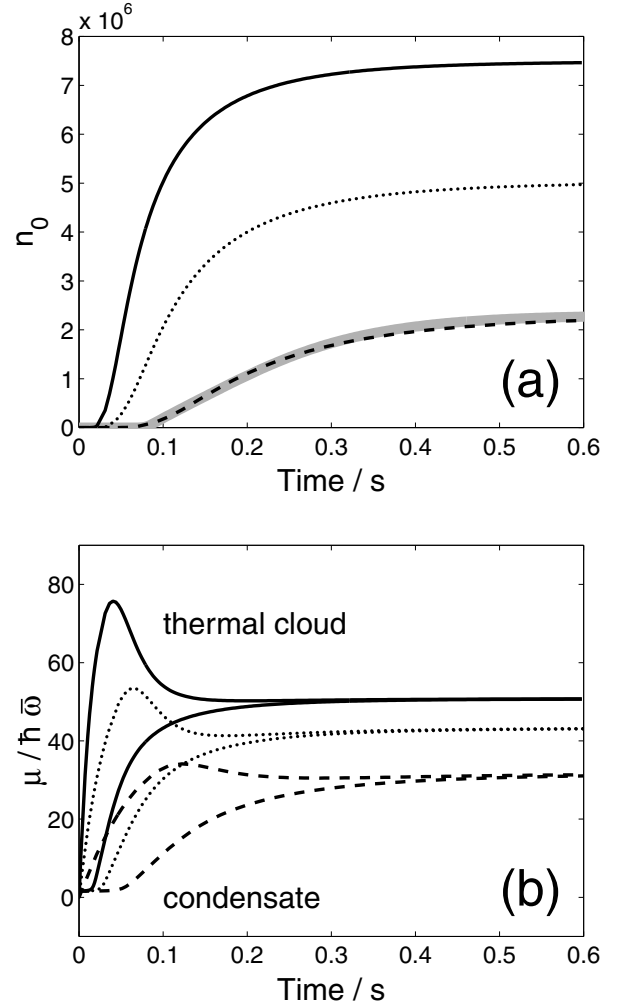


FIG. 9. Growth of a condensate with a final temperature of 590nK, starting from an uncondensed thermal cloud with $_{init} = 0$. Solid line 7.5×10^6 atoms, dotted line 5.0×10^6 atoms, dashed 2.5×10^6 atoms. The dashed line is for the same parameters as the lower temperature curves in [3], and the earlier model curve is shown as a grey curve in (a).

$n_0 = 10^6$	T_i (nK)	$N_i = 10^6$	$"_{cut}=h!$	Condensate fraction
2.3	692.5	29.6	4.07	0.095
5.0	794.6	44.7	2.91	0.179
7.5	897.9	64.6	2.29	0.239

TABLE III. Parameters for the formation of condensates at $T_f = 590$ nK from an uncondensed thermal cloud with $_{init} = 0$. The growth curves are presented in Fig. 9

a higher collision rate to begin with), but also they need to be truncated more severely, causing a larger difference in the chemical potentials, as seen in Fig. 9b. Thus instead of these effects negating each other as in the previous section, here they tend to reinforce one another. This causes the growth rate to be highly sensitive to the final number of atoms in the condensate for a fixed final temperature. This could have

implications for the comparison with experiment, where the uncertainty in the number of atoms in the condensate can be quite large (see [10] for further discussion of this point). For further comparison with the previous model, in Fig. 9a the dashed curve is for the same parameters as for the lower temperature results of [3], whose prediction is plotted in grey—as can be seen, the two methods are in very good agreement with each other for this choice of parameters.

F. The appropriate choice of parameters

In our computations we have taken some care to make sure that we can give our results as a function of the experimentally measured *final* temperature T_f and condensate number n_0 . Nevertheless, it can be seen from our results that this can give rise to counterintuitive behavior, such as the fact that under the condition of a given final condensate number, the growth rate seems to be largely independent of temperature, because of the cancellation noted in sect. V D. This counterintuitive behavior has its origin in the quite simple fact that with a sufficiently severe cut it is impossible to separate the process of equilibration of the vapor distribution to a quasiequilibrium from the actual process of growth of the condensate. In other words, the attempt to implement the “ideal” experiment in which a condensate grows from a vapor with a constant chemical potential and temperature cannot succeed with a sufficiently large cut. Under these conditions, the initial temperature differs quite strongly from the final temperature, and as well, the number of atoms required to produce the condensate is so large that the vapor cannot be characterized by a slowly varying chemical potential during most of the growth process.

G. Comparison with experiment

The most quantitative data available from [11] is in their Figure 5, in which results are presented as parameters extracted from fits to the simple growth equation. In [3] we took two clusters of data from this figure, at the extremes of the temperature range for which measurements were made, and compared the theoretical results with the fitted experimental curves. At the higher temperature of 830nK the results were in good agreement with experiment, but at 590nK they differed significantly, the experimental growth rate being about 3 times faster than the theoretical result.

We have performed the same calculations using the detailed model. The results for 830nK are presented in Fig. 6. and those for 590nK are presented in Fig. 9. There is a good match between the two theoretical models at *both* temperatures.

Thus, although we have shown that a significant speedup of the condensate growth can occur at higher condensate fractions, this cannot explain the discrepancy with the experimental results, for the measured values of temperature and condensate fraction. Nevertheless, the actual speedup observed is

of the order of magnitude of that achievable with a higher condensate fraction, and it is conceivable that the problem could be experimental rather than theoretical—a systematic error in the methodology of extracting the condensate number from the observed data could possibly cause the effect. For a realistic comparison to be made between experiment and theory, sufficient data should be taken to verify positively all the relevant parameters which have an influence on the results. Thus, one should measure initial and final temperatures, the final condensate number, the number of atoms in the vapor initially and finally, and the size of the “cut”.

VI. CONCLUSION

We have extended the earlier models of condensate growth [1–3] to include the full time-dependence of both the condensate and the thermal cloud. We have compared the results of calculations using the full model with the simple model, and determined that for bosonic stimulation type experiments resulting in a condensate fraction of the order of 10%, the model of [3] is quite sufficient.

However, for larger condensate fractions the depletion of the thermal cloud becomes important. We have introduced the concept of the effective chemical potential ϵ_e for the thermal cloud as it relaxes, and observed it to overshoot its final equilibrium value in these situations, resulting in a much higher growth rate than the simple model would predict. Thus we have identified a mechanism for a possible speedup that may contribute to eliminating the discrepancy with experiment.

We have also found that the results of these calculation can be qualitatively explained using ϵ_e and the simple growth equation (1). In particular, the rate of condensate growth for the same size condensate can be remarkably similar over a wide range of temperatures; in contrast, the rate of growth is highly sensitive to the final condensate number at a fixed temperature.

This model we have used in this paper eliminates all the major approximations in the calculation of condensate growth, apart from the ergodic assumption, whose elimination would require massive computational resources. In the absence of experimental data sufficiently comprehensive to make possible a full comparison between experiment and theory, this does not at present seem justified.

ACKNOWLEDGMENTS

M.J.D. would like to thank Keith Burnett for his support and guidance, Mark Lee for many useful discussions, and St. John’s College, Oxford for financial support. This work was supported by the Royal Society of New Zealand under the Marsden Fund Contracts PVT-603. and PVT-902

[1] C. W. Gardiner, P. Zoller, R. J. Ballagh and M. J. Davis, Phys. Rev. Lett. **79**, 1793 (1997)

[2] C.W. Gardiner, M.D. Lee, R.J. Ballagh M.J. Davis and P. Zoller, cond-mat/9801027 5 Jan 1998.

[3] C. W. Gardiner, M. D. Lee, R. J. Ballagh, M. J. Davis, and P. Zoller, Phys. Rev. Lett. **81**, 5266 (1997)

[4] In this paper will use the notation: QKI for [5], QKII for [6], QKIII for [7], and QKIV for [8] QKV for [9] QKVI for [10]

[5] C.W. Gardiner and P. Zoller, Phys. Rev. A **55**, 2902 (1997)

[6] D. Jaksch, C.W. Gardiner and P. Zoller, Phys. Rev. A **56**, 575 (1997)

[7] C.W. Gardiner and P. Zoller, Phys. Rev. A **58**, 536 (1998)

[8] D. Jaksch, C.W. Gardiner and P. Zoller, Phys. Rev. A **58**, 1450 (1997)

[9] C. W. Gardiner and P. Zoller, *Quantum Kinetic Theory V: Quantum kinetic master equation for mutual interaction of condensate and noncondensate*, cond-mat/9905087

[10] M. D. Lee and C. W. Gardiner, *Quantum Kinetic Theory VI: The Growth of a Bose-Einstein Condensate*, cond-mat/9912420

[11] H. J. Miesner, D. M. Stamper-Kurn, M. R. Andrews, D. S. Durfee, S. Inouye, and W. Ketterle, Science **279**, 1005 (1998)

[12] F. Dalfovo, S. Giorgini, L.P. Pitaevskii and S. Stringari, Rev. Mod. Phys. **71**, 463 (1999)

[13] E. Timmermans, P. Tommasini, and K. Huang, Phys. Rev. A. **55**, 3645 (1997)

[14] M. Holland, J. Williams, J. Cooper, Phys. Rev. A **55**, 3670 (1997).

[15] O. J. Luiten, M. W. Reynolds, J. T. M. Walraven, Phys. Rev. A **53**, 381 (1996), M.J. Davis, B.Sc. Honours thesis, University of Otago (1996).